Linear Rheology of Entangled Six-Arm and Eight-Arm Polybutadienes

Mohammad T. Islam, Juliani,* and Lynden A. Archer*

Department of Chemical Engineering, Texas A&M University, College Station, Texas 77843

Sunil K. Varshney

Polymer Source Inc., Dorval, PQ, Canada H9P 1G7

Received May 22, 2000; Revised Manuscript Received March 1, 2001

ABSTRACT: Relaxation dynamics of various model entangled six-arm (A_3-**A**-A_3) and eight-arm (A_3-**A**-A_2-**A**-A_3) polybutadiene melts are investigated using low-amplitude oscillatory shear and time-dependent step strain measurements. The frequency (time) and temperature range covered in these experiments are sufficiently broad to characterize the entire liquid-state relaxation spectrum of the materials. Several new findings about multiarm polymer dynamics are reported. First, the mean segmental relaxation time of multiarm polymers is a function of crossbar (**A**) molecular weight and polymer architecture. Second, for polymers with fixed arm (A) molecular weight, but variable crossbar molecular weight, terminal relaxation time (λ) and limiting shear viscosity (η_0) scale quite strongly with crossbar molecular weight M_b ($\lambda \sim M_b^{\sim 6.8-7}$, $\eta_0 \sim M_b^{\sim 8}$). When the crossbar tube length is renormalized by dilution of relaxed arms and the relaxation time and viscosity are rescaled to remove the inherent M_b dependence of segmental scale properties, these scaling exponents become closer to values expected for crossbar reptation in a dilated tube. Finally, relaxation dynamics of eight-arm A_3-**A**-A_2-**A**-A_3 polybutadienes are found to be quite different from those of six-arm A_3-**A**-A_3 polymers with comparable arm molecular weight. Specifically, the slowest relaxation mode in well-entangled eight-arm polymers appears to be dominated by Rouse-like fluctuation effects, which blur the transition from high-frequency arm to terminal backbone relaxation.

Introduction

Polymers with multiple long side chain branches have melt and solid-state properties that are remarkably different from their linear counterparts of comparable molecular weight.[1] Rheological investigations of model LCB polymers including multiarm stars,[2−4] comb polymers,[5,6] four-arm (A_2-**A**-A_2 or H-shaped),[7−9] and six-arm (A_3-**A**-A_3 (Figure 1))[10] polymers indicate that the number of arms, their length, length of the crossbar, and distribution of arms along the chain contour profoundly impact viscoelastic properties such as zero shear viscosity η_0, terminal relaxation time λ_0, and breadth of their relaxation spectra.

Graessley,[11] for example, measured the zero shear viscosity (η_0) of linear, four-arm, and six-arm star polyisoprenes with similar overall molecular weight, dissolved in tetradecane. At low solution concentrations the viscosity of the linear polymer was found to be higher than that of the branched ones. But as the polymer concentration was increased, a greater enhancement in solution viscosity was observed for star polymers than for the linear ones. Graessley's low-concentration results are quantitatively explained by the difference in radius of gyration of linear and branched polymers of comparable molecular weight ($\eta_0 = Kc^{1.5}(cgM_w)^a$). Specifically, the square of the ratio of the radius of gyration of a regular star and linear polymer, g, decreases with the number of branches, f, as $g = (3f - 2)/f^2$. The enhanced viscosity observed at high star concentrations cannot be explained in terms of structural differences alone. Instead, detailed knowledge of the effect of arm length on molecular friction and relaxation dynamics is required.

The relaxation spectrum for high molecular weight star polymers was first calculated by Pearson and Helfand.[3] These authors contended that the loss of orientation of entangled chain segments occurs via "breathing modes" of the arms and that the total stress after imposition of a step strain is proportional to the length of tube still unvisited by chain end. The resulting viscosity was found to depend exponentially on arm molecular weight (M_a), $\eta_0 \sim M_a^{1/2} \exp[\nu M_a/M_e]$, where $\nu = 15/8$ (experimentally obtained value was 0.6).

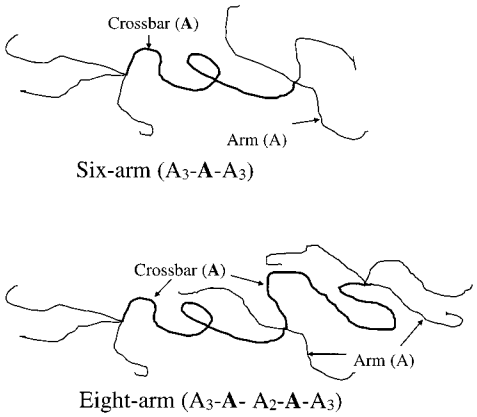

Figure 1. Molecular architecture of six-arm and eight-arm polybutadienes.

Ball and McLeish[12] considered the effect of relaxed outer arm sections on arm relaxation dynamics of star polymers. These authors argued that because the outermost arm segments relax much more quickly than segments closest to the branch point, they function as an effective solvent for the unrelaxed inner arm sections during the course of arm relaxation. The main effect is that the entanglement spacing is renormalized by the dilution process, $M_e(S_a) = M_{e0}/(1 - S_a/M_a)$. Here S_a is a contour variable that keeps track of the position, relative to the branch point, of relaxed arm segments. If the branch point is assumed to remain fixed during the

10.1021/ma000892n CCC: $20.00
Published on Web 07/31/2001

course of arm relaxation, an expression for η_0 can be obtained by integrating the relaxation modulus, $\eta_0 \sim (\nu M_a/M_{e0})^{-1} \exp[\nu M_a/3M_{e0}]$. Milner and Mcleish[3,4] further refined this picture to include a more realistic dependence of the diluted entanglement molecular weight on relaxed arm concentration and fast Rouse relaxation modes of outer arm segments, which significantly impact relaxation at early times. The improved analysis yields predictions for $G(t)$ and thereby G' and G'' that are in better accord with experiment.[3,4]

In a study employing H-shaped A_2-**A**-A_2 polystyrene, Roovers found that the zero shear viscosities (η_0) of low molecular weight materials are the same as those of linear polymers of comparable molecular weight.[8] At high polymer molecular weights, however, the viscosity of an H-shaped polymer is generally larger than that of a linear one of the same molecular weight. Roovers' viscosity results for low molecular weight polymers can be readily explained in terms of the similarity of the molecular friction coefficients ζ_P of the two polymer types: $\zeta_{P,L} = \zeta_{P,H} \sim N\zeta_m$, ($\eta_0 \sim \zeta_P/b$), where ζ_m is a segmental friction coefficient assumed to be independent of polymer molecular weight, N is the number of monomer units in the polymer chain, b is the statistical segment length, and the subscripts L and H indicate linear and H-shaped polymer, respectively. As was the case for the star-shaped polymers, however, interpretation of the high molecular weight viscosity results requires additional information about the effect of arm (A) friction and dynamics on crossbar (**A**) relaxation.

As a first guess, one might suppose that when arms are long enough to entangle, they will increase frictional drag between neighboring H-polymer chains, which enhances viscosity. The presence of an entangled linear crossbar in H-shaped materials also explains the greater enhancement of viscosity seen in direct comparisons with star polymers with comparable molecular weight.[8]

Similar ideas may be used to describe linear rheology of more complex topologies such as entangled multiarm, comb, and pom-pom polymers of the type considered in the present study. In these systems dynamics of the arms can be treated in a similar way to those of star arms because the branch point can be regarded as fixed on time scales of arm relaxation. Yurasova et al.,[6] for example, studied stress relaxation dynamics in entangled comb polymer melts by considering retraction of the arms as diffusion of the chain end in a mean-field effective potential. By taking into consideration constraint release via tube dilation, these authors predicted two qualitatively different types of long-time behavior, depending on whether the comb backbones are self-entangled or not. When backbones are mutually unentangled, the Rouse model can be used for long time stress relaxation in a high-friction medium with all the friction effectively located at the branch points. The Rouse relaxation time can be expressed as

$$\tau_R \sim (\text{no. of branch points} - 1)^2 (\text{longest relaxation time of arms}) \quad (1)$$

For mutually entangled backbones, the final stress relaxation will be via reptation in a wider tube with a relaxation time,

$$\tau_{rep} \sim (\text{no. of entanglements})^2(\text{no. of branch points})(\text{longest relaxation time of arms}) \quad (2)$$

The limiting or zero-shear viscosity in the entangled case is related to τ_{rep} by $\eta_0 \approx G_e\tau_{rep}$, where G_e is the entanglement modulus in the wider tube.

Likewise, in the case of the multiarm, pom-pom polymers coupling between arm (branch) and backbone dynamics lasts well beyond arm relaxation. Thus, when arms segments are fully relaxed, the backbone can be approximated as a linear chain trapped in a wider, diluted tube and retarded by friction blobs attached at the branch points.[3] The terminal or escape time τ of a polymer with κ equal-sized branches per chain is therefore $\tau \approx L_b^2/(kT/\zeta_T) = (N_b/N_{eb})^2\tau_m(N_{eb}N_b + \kappa\tau_{arm}/\tau_m)$, where $N_{eb} = N_{eb0}/\phi_b^{\alpha}$, ζ_T is the tube friction coefficient, and $\phi_b = S_b/(\kappa S_a + S_b)$. $S_a = N_a/N_{ea0}$ and $S_b = N_b/N_{eb0}$ are the entanglement density of the arm and backbone sections, and $\alpha = {}^4/_3$.[13] The limiting shear viscosity $\eta_0 \approx G_B\tau$ can be computed from τ and the modulus $G_B = \phi_b^{\alpha+1}G_N$ of the dilated network enmeshing the polymer backbone. The key new results are: (i) provided arms are long enough to entangle, both the terminal viscosity and relaxation times are exponential functions of arm molecular weight; and (ii) the plateau modulus in the terminal regime is not strictly a property of the entangled polymer network (cf. linear polymers) but is instead a function of arm and crossbar length.

A different, though essentially phenomenological approach for evaluating linear relaxation dynamics in branched polymers recognizes that the main new contribution is coupling between crossbar and arm dynamics. In this method, the broadening of the relaxation spectrum resulting from such coupling may captured, qualitatively, by the exponent (β) of the Kohlrausch−Williams−Watts (KWW) stretched exponential function[14] (eq 3). According to this function, time-dependent properties such as the modulus $G(t)$ can be represented using an equation of the form

$$\varphi(t) \propto \exp(-(t/\lambda)^{\beta}) \quad (3)$$

Although this expression for $\phi(t)$ was developed to describe segmental dynamics in polymers, it can be used in connection with Ngai's coupling model[15] to describe dynamics in the terminal regime.[14] β can be related to the coupling parameter (n) ($n = 1 - \beta$). For highly entangled linear polymers, the glassy and terminal relaxation processes are completely separated. This is evidenced by two distinct peaks in the loss modulus (G'') obtained from linear oscillatory shear rheometry for a linear polymer (Figure 3). The stretch exponents for the terminal and glassy regions, β_η and β_α, respectively, can therefore be obtained by fitting eq 1 for both the peaks. The two different shift factors in the terminal (β_η) and glassy zone (β_α) indicate that molecular processes are coupled differently to their environment and therefore shift differently with temperature, which causes deviation from thermorheological simplicity.[16] In the case of multiarm polymers, another stretch exponent (β_{arm}) can be obtained from the G'' peak corresponding to the arms relaxation.

In the present study, we investigate relaxation dynamics and linear rheological behavior of well-defined, entangled six-arm and eight-arm polymers. We focus on the influence of crossbar molecular weight on relaxation dynamics of a series of polymers with nearly constant arm molecular weight. These multiarm polymer systems allow several fundamental questions about branched polymer physics to be addressed. First, the

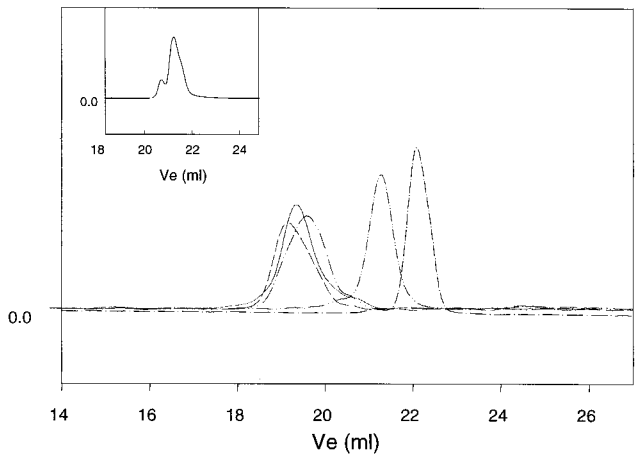

Figure 2. Size exclusion chromatography (SEC) profiles of sample P1508_6 and P1508_8. The peaks from right to left correspond to (i) branch: M_n = 20 200, M_w = 21 000, M_w/M_n = 1.04; (ii) crossbar (before terminating with $SiCl_4$): M_n = 42 000, M_w = 45 800, M_w/M_n = 1.09; (iii) six-arm (P1508_6) with respect to linear polybutadiene standards: M_n = 152 000, M_w/M_n = 1.13; (iv) six-arm (P1589) with respect to linear polybutadiene standards: M_n = 175 000, M_w/M_n = 1.17; (v) eight-arm (P1508_8) with respect to linear polybutadiene standards: M_n = 215 000, M_w/M_n = 1.13. The SEC profile of the crossbar after terminating with $SiCl_4$ is provided in the inset. The smaller of the two maxima is due to elution of a higher molecular weight crossbar fraction with approximately double the molecular weight of the larger peak fraction.

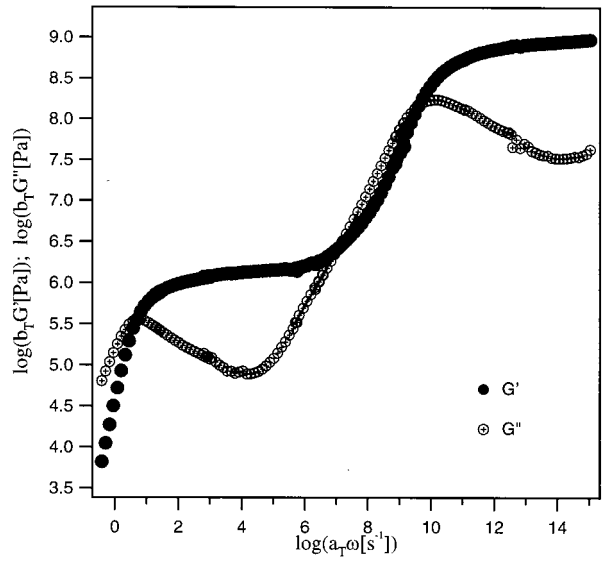

Figure 3. Oscillatory shear properties of a linear 1,4-polybutadiene (sample PB161).

effect of systematic variations of crossbar molecular weight on rheological properties provides an answer to the most important question: Can the long-time dynamics of such an unwieldy architecture be reptational diffusion? Second, because multiarm samples with short and long crossbar lengths are used in the study, multiarm polymer dynamics for marginally entangled (Rouse-like, in the dilated tube) and well-entangled crossbars can be investigated. Finally, fundamental understanding of dynamics of polymers with model branched architectures should in principle lead to better descriptions of properties of more complex commercial branched polymers. Rheological measurements employing model eight-arm polymers with an A_3-**A**-A_2-**A**-A_3 architecture (Figure 1) allow us to evaluate this hypothesis for a limited number of systems. These last polymers offer a closer, but still imperfect, topological resemblance to commercial branched polymers and allow us to determine the range of applicability of theoretical constructs like the mean-field tube and reptation for more complex multiarm polymer architectures.

Experimental Section

Materials. Various narrow molecular weight distribution (MWD) six-arm A_3-**A**-A_3 1,4-polybutadienes with fixed arm molecular weight, but variable crossbar molecular weight, were synthesized using anionic living polymerization. Detailed synthesis procedures for creating monofunctional living arms, difunctional crossbars, and methods for linking them to produce A_3-**A**-A_3 polybutadienes with high 1,4-microstructures are described in detail elsewhere.[10] Synthesis of narrow MWD eight-arm (A_3-**A**-A_2-**A**-A_3) polybutadienes was performed using a two-step procedure illustrated below and shown in Scheme 1.

(i) Synthesis of α-ω-Bis(trichlorosily)polybutadiene and α-ω-Bis(trichlorosily)dichlorosilylpolybutadiene Central Block. The detailed synthesis of well-defined architecture of α-ω-bis-(trichlorosily)polybutadiene central block has been described previously.[10] For the synthesis of α-ω-bis(trichlorosily)polybutadiene that contains a low fraction of (around 10−15%) α-ω-bis(trichlorosily)dichlorosilylpolybutadiene (bearing octachlorosilane functionality) a slight modification of the procedure presented in ref 10 was used: α-ω-dilithio macroanions of polybutadiene were end-capped with diphenylethylene (around 20% less than the stoichiometric amount with respect to the initiator). The solution was then transferred to a large excess of vigorously stirred, purified silicon tetrachloride (2000 molar excess with respect to the initiator). The SEC profile of the product is shown in the inset to Figure 2 and indicates a bimodal size distribution. The higher molecular weight fraction was found to comprise around 10−15% of the total product, as determined from the area of the SEC profile. The molecular weight of the higher molecular weight fraction was found to be approximately double that of the main counter molecular species. The obtained α−ω-bis(trichlorosily)polybutadiene and/or mixture with α−ω-bis(trichlorosily)dichlorosilylpolybutadiene block was purified by removing excess of $SiCl_4$ under vacuum followed by freeze-drying in purified dry benzene.

(ii) Synthesis of Polybutadiene Sidearm -A and Linkage. Polybutadiene was prepared in a specially constructed 250 mL round-bottom flask connected through its sidearm by a break-seal to another 250 mL flask containing purified α−ω-trichlorosilypolybutadiene and/or its mixture with the α−ω-bis(trichlorosily)dichlorosilylpolybutadiene block. Polymerization of purified butadiene monomer was initiated by *sec*-BuLi in benzene at room temperature and left overnight. The obtained living polybutadieneyllithium was added (10 times molar excess with respect to α−ω-trichlorosilylpolybutadiene and/or mixture with α−ω-bis(trichlorosily)dichlorosilylpolybutadiene block) to α−ω-trichlorosilylpolybutadiene through the sidearm. The linking reaction was performed at 35 °C for over 76 hours. The final A_3-**A**-A_3 *six-arm* and A_3-**A**-A_2-**A**-A_3 *eight-arm* polybutadienes were separated from the unlinked polybutadiene homopolymer by repeated fractionation in toluene/methanol at 30 °C. Separation of eight-arm architecture of high purity (minor faction) from the six-arm fraction (major fraction) required numerous repeat selective solvent−nonsolvent fractionations. For example, to obtain about 2−3 g of purified eight-arm architecture, about 80−100 g of the crude polymer was required. Various multiarm polymers were synthesized with different degrees of polymerization for both the central **A** and terminal arm A blocks. Figure 2 illustrates typical SEC profiles of some of these materials.

Sketches of the six-arm and eight-arm polymer architectures used in the study are provided in Figure 1. Molecular parameters for these materials are summarized in Table 1. Molecular weight information was obtained from SEC profiles

Scheme 1. Schematic Methodology Used To Synthesize A_3-A-A_3 (Six-Arm) and A_3-A-A_2-A-A_3 (Eight-Arm) Architectures

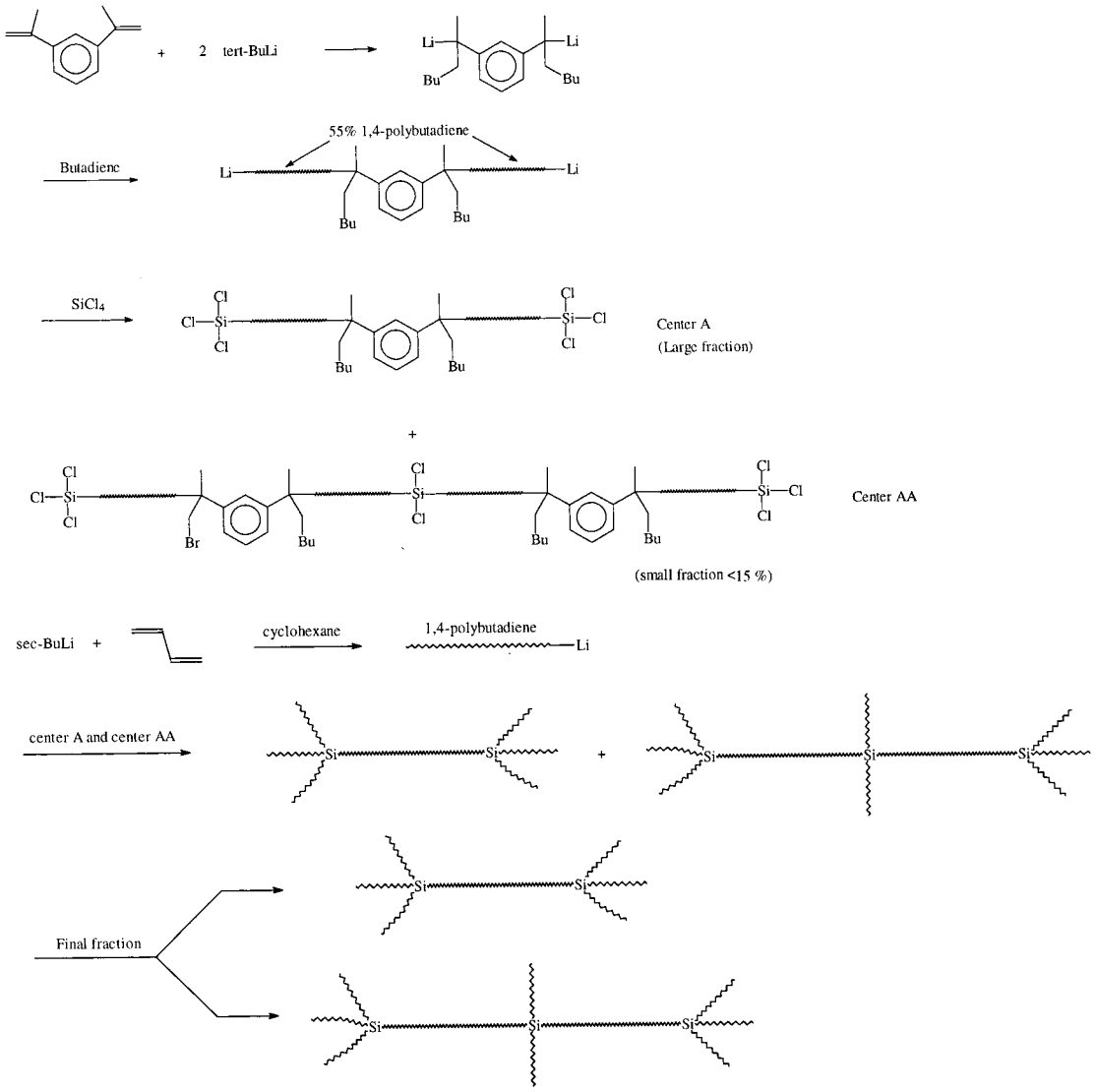

Table 1. Molecular Parameters for Linear and Multiarm Polybutadienes

sample	type	$\bar{M}_n \times 10^{-4}$ of crossbar[a]	$\bar{M}_n \times 10^{-4}$ of arm[b]	$\bar{M}_w/\bar{M}_n$ of arm	$\bar{M}_n \times 10^{-4}$ of polymer	$\bar{M}_w/\bar{M}_n$ of polymer
P1508_8	eight-arm	4.2	2.02	1.04	21.5	1.13
P1531_8	eight-arm	4.2	2.04	1.03	23.0	1.12
P1508_6	six-arm	4.2	2.02	1.04	15.2	1.13
P1531_6	six-arm	4.2	2.04	1.03	15.4	1.13
P1589	six-arm	8.3	2.00	1.04	17.5	1.17
P1207	six-arm	9.07	1.96	1.03	21.53	1.10
P1625	six-arm	14.0	2.08	1.06	23.25	1.15
PB129[b]	linear				12.94	1.03
PB1739[b]	linear				1.00	1.04
PB1958[c]	linear				1.07	1.11

[a] H NMR analysis indicates 55% 1,4 addition. [b] H NMR analysis indicates 92% 1,4 addition. [c] H NMR analysis indicates 87.5% 1,2 addition.

using linear polystyrene standard. To ascertain the effect of branching on retention times and molecular weights, SEC characterization of a few selected samples as supplemented by on-line multiangle light-scattering measurements. For the six-arm sample labeled P1508_6, M_w values obtained from light scattering and SEC were 195 800 and 171 800, respectively, suggesting the ratio of radii of gyration, g ($g = \langle R_g^2\rangle_{branched}/\langle R_g^2\rangle_{linear}$) to be 0.88. The corresponding values for the eight-arm polybutadiene designated P1508_8 were 296 500 and 243 000, indicating a g value of 0.82. For another six-arm sample (P1531_6), $g = 0.89$. The values obtained for g are typical of the target branched structures, confirming the architecture suggested by the synthesis scheme.

In Table 1, the variability in arm molecular weight for several of the multiarm polymer samples is seen to be within the uncertainty of determining the molecular weight of the unlinked arm, indicating that changes in crossbar molecular weight will have a much greater effect on rheological properties. H NMR analysis was performed to determine the microstructure of the arm and functionalized crossbar materials prior to linkage. Results indicate 55% 1,4 addition for the crossbars and >92% 1,4 addition for the arms. The entangle-

Table 2. Rheological Parameters for Linear and Multiarm Polybutadiene Samples

sample	ω_c [1/s]	$\omega_{min} \times 10^{-4}$ [1/s]	$G_N \times 10^{-6}$ [Pa]	$\eta_0 \times 10^{-4}$ [Pa s]	m	$\omega_{max} \times 10^{-8}$ [1/s]	$G_g \times 10^{-8}$ [Pa]
P1531_8	53.4	9.74	1.10	2.1	0.64	6.6	0.545
P1531_6	14.0	4.97	1.02	8.76	0.67	21.9	0.88
P1508_8	23.5	4.41	0.98	2.82	0.71	8.0	1.31
P1508_6	12.6	4.25	1.02	8.43	0.68	13.9	1.26
P1589	0.00186	1.89	0.89	3980	0.63	2.49	1.01
P1207	0.0015	0.84	0.92	6270	0.67	1.75	1.14
P1625		0.2	0.80		0.67	1.12	1.28
PB161	5.0	1.46	1.01	15.62	0.69	52.8	9.82
PB129	7.4	2.84	1.03	8.45	0.63	56.2	8.52
PB1739	33090			0.0038	0.59	50.3	10.9
PB1958	391			0.272	0.67	4.2	8.8

Table 3. Effect of Arm Relaxation on Crossbar Entanglement Density

sample	ϕ_b	$N_b\phi_b^{\alpha}/N_{beo}$	$\omega_{B,min}$ [1/s]	$G_B \times 10^3$ [Pa]	G_B/G_N, exptl	$\phi_b^{\alpha+1}$
P1531_8	0.340	10.6				
P1531_6	0.256	3.64				
P1508_8	0.342	10.7				
P1508_6	0.257	3.64				
P1589	0.409	13.42	0.09	98.3	0.110	0.124
P1207	0.435	15.92	0.10	143.0	0.155	0.143
P1625	0.529	31.87	0.02	141.1	0.176	0.226

ment molecular weight (M_e) of 1,4-polybutadiene is reported to be 1543 g/mol[17] and 2100 g/mol.[18] For a 60% 1,4 and 40% 1,2 polybutadiene M_e is reported to be 1880 g/mol.[17] Thus, excluding the arm dilution effects envisaged by theory, arms and crossbars of the polymers used in this study can be considered well entangled ($M_{arm}/M_e > 12$, $M_{crossbar}/M_e > 22$).

Linear Rheology Experiments. Linear viscoelastic properties of multiarm polymers were characterized by small-amplitude oscillatory shear rheometry and step shear measurements. Oscillatory shear measurements were performed over a temperature range of −90 to 150 °C using a Paar Physica Universal dynamic spectrometer (UDS200), equipped with a TEK 600 temperature controller, and a Modular Compact rheometer (MCR300) with a CTD600 temperature controller. Temperature regulation was performed using liquid nitrogen. For lower temperature measurements, precaution needs to be taken to eliminate ice condensation on the moving parts of the rheometer. At higher temperatures, an argon blanket was used to prevent sample oxidation during rheological experiments. Stainless steel cone-and-plate (15 mm diameter, gap angle 1.6°; 15 mm diameter, gap angle 6.5°) and parallel plate (10, 8, and 6 mm diameter) rheometer fixtures were used in these measurements. Strain amplitudes varied from 0.025% at low temperatures and high frequency (i.e., near the glassy or softening zone) to 150% at high temperatures and low frequency (in the terminal zone). To ensure linearity in the oscillatory shear and step strain experiments, measurements at all temperatures and frequencies were repeated at progressively lower strain amplitudes until material functions (e.g., G', G'', and $G(t)$) manifested no change in response with changing strain.

Several rheological parameters obtained from these experiments are summarized in Table 2 for linear and multiarm 1,4-polybutadienes. Plateau moduli G_N of all samples were estimated as their storage modulus (G') value at the frequency (ω_{min}), where the loss modulus (G'') displays a local minimum (i.e., just before the upturn in G'' in the segmental region).[18] The crossover frequency ω_c was determined from the interception of G' and G'' just prior to the terminal regime. The frequency (ω_{max}) at which G'' shows a maximum in the segmental region, the glassy modulus, G_{glassy}, and the average slopes of G' and G'' in the glass transition zone are also presented in Table 2. For some of the multiarm polymers, there is a second minimum in G'' corresponding to backbone or crossbar relaxation. This frequency ($\omega_{B,min}$) and the corresponding storage modulus G_B values are also provided in Table 3.

Zero shear viscosities (η_0) were determined from the slope of the G'' in the terminal region: $\eta_0 = \lim_{\omega\to 0}[G''(\omega)/\omega]$. Determination of η_0 by this method was not possible for all samples because the terminal frequency region of some materials were inaccessible to our experiment, even at 150 °C (the maximum temperature at which an argon environment was deemed effective at preventing sample oxidation). For these samples, relaxation moduli $G(t)$ determined from low-amplitude step strain experiments were used to determine η_0, $\eta_{0,step} = \int_0^\infty G(t)\,dt$. Other linear viscoelastic material properties can also be determined from these experiments, $J_{e0,step} = (1/\eta_{0,step})^2 \int_0^\infty tG(t)\,dt$ and $\lambda_{0,step} = \eta_{0,step} J_{e0,step}$.[18] A second estimate of the terminal relaxation time for each of the multiarm polymers was obtained from the long time slope of the semilogarithmic plot of $G(t)$ vs time. In systems where the terminal zone was accessible to oscillatory shear measurements, rheological data obtained from oscillatory shear and from step strain compare favorably (Table 5).

Results and Discussion

Master plots of storage G' and loss G'' moduli of all polymers are presented in Figures 3−6. These plots cover a frequency range of almost 14 decades and were constructed from data at discrete temperatures in the range −90 to 150 °C using horizontal (a_T) and vertical (b_T) shift factors [$G'(\omega,T) = b_T G'(a_T\omega,T_0)$; $G''(\omega,T) = b_T G''(a_T\omega,T_0)$]. The reference temperature for construction of all master curves is 25.5 °C. Data from a linear polybutadiene melt (PB161) with a number-average molecular weight $M_n = 161\,600$, which is close to the overall molecular weights of P1531_6 and P1508_6, is also included to facilitate comparison with typical linear polymer behavior.

As expected, the linear polybutadiene shows two dominant relaxation modes (two well-defined G'' maxima, see Figure 3). One maximum is observed at high frequencies in the transition zone between the rubbery and glassy plateaus and is attributable to long-range segmental motions. The other low-frequency loss maximum occurs at the end of the rubbery plateau and is attributable to long-range translational motion of entire molecules. The rubbery plateau spans more than 4 decades of frequency and is identifiable by a nearly constant storage modulus, $G' = G_N \approx 1.1$ MPa. Using the relationship $M_e = 0.8\rho N_A kT/G_N$,[18] the entanglement molecular weight for this polymer may be estimated, $M_e = 1822$ g/mol. The ratio of frequency at which G'' displays a minimum to the crossover frequency can also be estimated from the data to be 2.94×10^3, which is more than 10 times the ratio of reptation and longest Rouse relaxation times ($\tau_{rep}/\tau_{Rouse} \approx 3M/M_e = 266$). Comparison of $\omega_{min}/\omega_c = 3.84 \times 10^3$ and $3M/M_e = 212$ for a second entangled linear 1,4-polybutadiene (PB129) confirms that it is incorrect even to seek an order of magnitude estimate of τ_{Rouse} from the location of the low-frequency loss minimum.

Table 4. Comparison of Longest Relaxation Time (λ_0) with Crossover Time (τ_c) and Ratio of Longest Relaxation Modulus (G_{long}) to G_N with Dynamic Dilution Values

sample	J_{e0} [Pa^{-1}]	λ_0 [s] ($\approx\eta_0 J_e^0$)	τ_c [s] ($\approx \omega_c^{-1}$)	G_{long} [Pa] ($\approx 2.4/J_e^0$)	G_{long}/G_N	$\phi_b^{\alpha+1}$
P1508–8	1.58×10^{-4}	4.45	0.0425	15124	0.0154	0.082
P1531–8	2.72×10^{-4}	5.70	0.0187	8816	0.0080	0.081
P1508–6	1.02×10^{-4}	9.63	0.0794	23628	0.023	0.042
P1531–6	1.08×10^{-4}	9.51	0.0714	22106	0.022	0.042
P1207	3.48×10^{-5}	2185.0	667.5	68869	0.077	0.143
PB129	5.64×10^{-6}	0.477	0.135	0.43×10^6		
PB1739	2.34×10^{-6}	8.79×10^{-5}	4.20×10^{-5}	1.02×10^6		
PB1958	4.66×10^{-6}	0.01269	0.0048	0.50×10^6		

Table 5. Terminal Relaxation Times and Zero Shear Viscosities Determined from Low-Amplitude Oscillatory Shear and Step-Shear Relaxation Experiments

sample	$J_{e0} \times 10^4$ [Pa^{-1}]	$J_{e0,step}$ [Pa^{-1}]	η_0 [Pa s]	$\eta_{0,Rep}$ ($\sim G_{Rep}\tau_{Rep}$) [Pa s]	$\eta_{0,step}$ [Pa s]	λ_0 [s]	$\lambda_{0,step}$ [s]	$\lambda_{d,step}$ [s]
P1531–8	2.72	4.4×10^{-4}	2.1×10^4		2.56×10^4	5.7	11.3	39.1
P1508–6	1.02	8.3×10^{-5}	8.4×10^4		1.04×10^5	9.63	8.6	18.2
P1207	0.35	3.0×10^{-5}	6.3×10^7	6.33×10^7	3.89×10^7	2185	1165	7250
P1589		1.57×10^{-5}		3.87×10^7	5.10×10^7		803	5263
P1625		1.50×10^{-5}			4.09×10^9		60900	110656

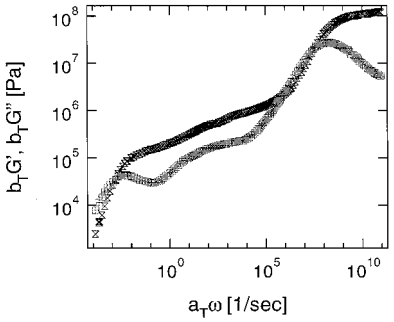

Figure 4. Oscillatory shear properties of an A_3-**A**-A_3 1,4-polybutadiene with high crossbar molecular weight (sample P1207).

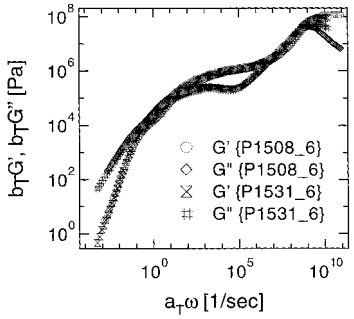

Figure 5. Dynamic moduli of multiarm polymers with similar arm and crossbar length (samples P1508–6 and P1531–6).

The width of the plateau region, $\Delta\omega_e$, is however consistent with expectation from theory ($\Delta\omega_e = \tau_{rep}/\tau_e \approx 3(M/M_e)^3$) to within a factor of 2 for both PB161 and PB129. The high-frequency maximum in G'' ($\omega_{max} = 6.3 \times 10^9$ s^{-1}) for PB161 provides an estimate for the mean segmental relaxation time, $\tau_m = 0.16$ ns. This value is also within a factor of 2 of the theoretical result, $\tau_m \approx \pi^2\tau_{rept}(N_e/N)^{1.5}(1/N^2) = 0.27$ ns or $\tau_m \approx \pi^2\lambda_0(N_e/N)^{1.5}(1/N^2) = 0.59$ ns, with an empirical correction to the molecular weight exponent to account for contour length fluctuations. Here we have used the approximation $\tau_{rep} \approx \omega_c^{-1}$, which generally underpredicts the reptation time by a factor of about 3; for the second case there is no such approximation. The equivalent estimate for PB129 is $\omega_{max} = 5.6 \times 10^9$ s^{-1} ($\tau_m = 0.18$ ns), which is again seen to be comparable with the value $\tau_m \approx 0.39$ ns estimated from τ_{rep}.

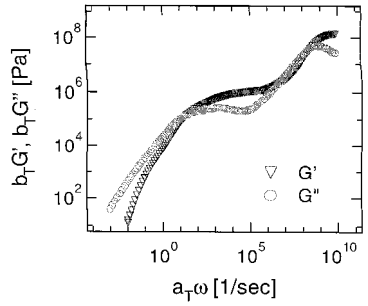

Figure 6. Storage and loss moduli of eight-arm (A_3-**A**-A_2-**A**-A_3 architecture) polybutadiene (sample P1508–8).

Unlike PB161, the multiarm polymers show at least three different relaxation regions. Dynamics in each of these regions reveal important differences between linear and multiarm polymers and even among multiarm polymers themselves. A high-frequency G'' peak is apparent in the transition region between the rubbery and glassy regimes (Figures 4−6). The magnitude of the loss maximum is, however, about 3−4 times lower than in PB161, and the location of the maximum (ω_{max}) is shifted to lower frequency for the multiarm materials (Table 2). The size of the frequency shift shows a clear, but unexpected, dependence on crossbar molecular weight and polymer architecture. For polymers with large crossbar molecular weights (P1589, P1207, P1625), the shift is large and segmental relaxation times ($\tau_m \sim \omega_{max}^{-1}$) range from 4 to 9 ns, which are closer to the τ_m values estimated for PB1958 a material with approximately 88% 1,2-polybutadiene content than with those observed for dominantly 1,4-polybutadienes. Segmental relaxation times observed for six-arm polymers with the lowest crossbar molecular weights (e.g., for P1531–6 and P1508–6, $\tau_m = 0.55$ and 0.7 ns, respectively) are in closer accord with results for 1,4-polybutadienes, indicating that the higher vinyl content of the crossbars could be to blame for the variability observed in τ_m.

The apparent increase in segmental relaxation time with increasing crossbar molecular weight is clearly seen in Figure 7a−b, where τ_m is plotted against inverse of crossbar number-averaged molecular weight for the six-arm polymers, and vs crossbar volume fraction for all polymers studied. It is apparent from Figure 7a that

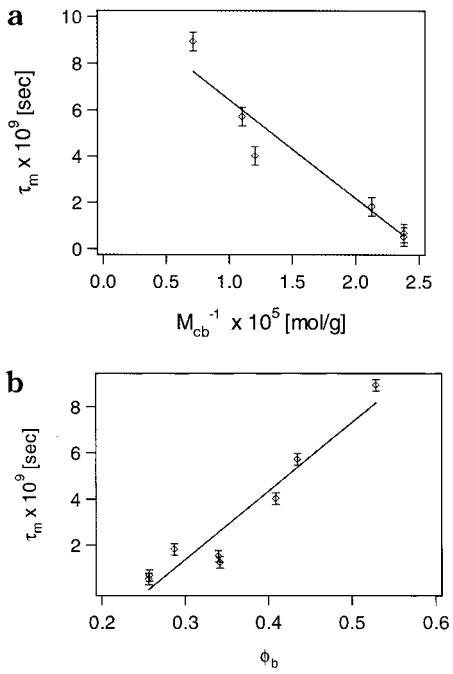

Figure 7. (a) Influence of crossbar molecular weight on mean segmental relaxation time of A_3-**A**-A_3 1,4-polybutadienes. (b). Effect of crossbar volume fraction on segmental relaxation time of all multiarm polymers.

an approximate power-law scaling relationship $\tau_m \sim 1/M_{nb}$ fairly summarizes the experimental observations. Figure 7b suggests a linear scaling relationship, $\tau_m \sim \phi_b$, for the multiarm materials as a group. The relationship $\tau_m \sim 1/M_{nb}$ is of the same form as the expression connecting glass transition temperature (T_g) and M_n of linear polymers ($T_g \sim 1/M_n$), suggesting that the either a higher fraction of chain ends or lower vinyl content of multiarm polymers with shorter crossbars may be the source of the experimental observations. A similar trend toward higher segmental friction coefficient, ζ_m ($\tau_m = b^2\zeta_m/kT$), with increasing polymer molecular weight, was reported over 20 years ago for linear poly(vinyl acetate) polymers with molecular weights below 4×10^5 g/mol.[19]

At frequencies below ω_{max}, G' and G'' are nearly equal to each other and manifest similar power-law dependencies on frequency $G' \approx G'' \sim \omega^m$ for all multiarm materials studied. Both observations are consistent with a transition from segmental to Rouse dynamics of entire molecules. The power-law frequency exponents are, however, substantially larger than the Rouse value of 0.5 (see Table 2). These exponents are in fact more consistent with Zimm-like dynamics, which raises obvious questions about the microscale mixing of the dominantly 1,4-polybutadiene arms and the moderately 1,4-crossbars. To pursue this point further, power-law slopes observed in low molecular weight polybutadienes with variable microstructures (PB161, PB1739, and PB1958) were investigated. The experimental results are also provided in Table 2. It is apparent from the data that even linear polymers with dominantly 1,4- (PB161 and PB1739, >92% 1,4-) and dominantly 1,2- (PB1958, 87.5% 1,2-) microstructures manifest power-law frequency exponents higher than the usual values for free Rouse chains, indicating the crossbar/arm microscale incompatibility is likely not the source of the Zimm-like power law scalings observed in the transition zone.

At frequencies below the power-law "Rouse" regime, a well-defined minimum is apparent in G''. The corresponding plateau in G' is neither as well-defined nor as broad as the storage modulus plateau observed for PB161. For all multiarm polymers investigated, the storage as well as loss moduli in this regime in fact appear to collapse onto a single curve, indicating that arm relaxation dominates dynamics. The slope of the G' plateau is found to be slightly greater for multiarm polymer samples with lower crossbar molecular weight. This dependence of arm relaxation rate on crossbar length is likely a consequence of coupling between fast arm and slow crossbar dynamics. Such coupling is consistent with a picture of mobile arms diffusing in a fixed network of crossbars and results in slowing down of arm dynamics.[1]

At even lower frequencies a second Rouse-like dynamic regime is accessed. In multiarm polymers with low crossbar molecular weights (P1508 and P1531 series), storage and loss moduli are again similar in magnitude over a range of frequencies (Figure 5). For higher crossbar molecular weights (P1132, P1207, P1589, and P1625), G' and G'' run parallel to each other for a range of frequencies, but G' is always a factor of about 5 times larger than G'' (Figures 4 and 9b). These observations can be explained in terms of the dynamic dilution argument proposed by Ball and McLeish.[7,12] Specifically, the second Rouse-like dynamic regime is accessed when arm relaxation is nearly over, i.e., when arm retraction reaches all the way to the branch point. Beyond that point, crossbar diffusion is the only important relaxation process. Since the relaxed arms can sample all possible configurations in the time required for crossbars to diffuse a distance of order an entanglement radius, arms function as an effective solvent for the crossbar and dilute its entanglement state. Crossbar relaxation should therefore progress by a series of diffusive hops in a dilated tube of diameter $a^* = a/\phi_b^{\alpha/2}$, where a is the undiluted tube diameter and ϕ_b is the mean volume fraction of the crossbar. The effective friction coefficient experienced by the crossbar during a single branch point hop is approximately the total drag arms experience in translating a distance equal to the size of the hop, $\zeta_{br} \approx j\zeta_{arm} = jkT\tau_{arm}/a^{*2}$, where j is the number of arms per branch point. The overall frictional drag per crossbar chain is therefore $\zeta_T \approx (N_b\zeta_m + n\zeta_{br},)$, where n is the number of branch points per crossbar. The time τ required for a crossbar to escape its primitive tube by this impulsive reptation motion is then $\tau \approx L_b^2/(kT/\zeta_T) = (N_b/N_{eb})^2\tau_m$ $(N_{eb}N_b + \kappa\tau_{arm}/\tau_m)$, where $N_{eb} = N_{eb0}/\phi_b^{\alpha}$ and $\kappa = jn$.

If the renormalized degree of entanglement of the crossbar is too low [$N_b\phi_b^{\alpha}/N_{eb0} \sim 1$] (as is the case for P1508–6 and P1531–6 from Table 3), relaxation dynamics should be physically similar to those of a slowed-down Rouse chain. This expectation is in fact consistent with experimental observation, except the power-law frequency exponents are again substantially larger than the typical Rouse value of 0.5 (between 0.58 and 1.0). When the renormalized entanglement density [$N_b\phi_b^{\alpha}/N_{eb0} > O(1)$] is high, as in the case of samples P1207, P1589, and P1625, crossbar relaxation is anticipated to progress in a mean-field tube. This point is supported by the fact that a second G'' minimum is apparent prior to the transition to terminal behavior. This loss minimum is, however, neither as sharp nor as deep as the

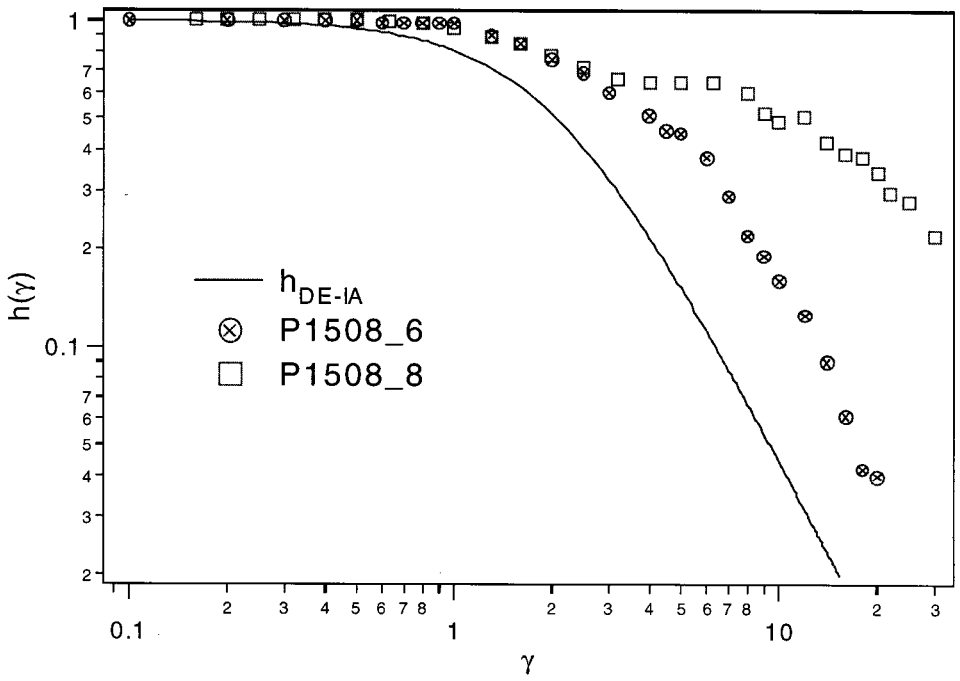

Figure 8. Step shear damping function $h(\gamma)$ for one six-arm (P1508_6) and one eight arm (P1508_8) materials. Damping function determined from the Doi−Edwards theory is included for comparison.

corresponding minimum observed for PB161 (Figure 3), indicating that many more relaxation modes are available to the crossbar even though its motion is restricted by entanglements with its neighbors. The storage moduli G_B corresponding to the minimum in G'' are presented in Table 3 for P1589, P1207, and P1625. These moduli values provide a direct test of the dynamic dilution argument. Specifically, if the relaxed arms dilate the crossbar tube, as claimed, the ratio G_B/G_N should be equal to $\phi_b^{\alpha+1}$, where $\beta' = \alpha + 1 = {}^7/_3$. The experimentally obtained values of the ratio G_B/G_N and the calculated values of $\phi_b^{\alpha+1}$ are provided in Table 3. Considering the uncertainty in the actual values of ϕ_b and β', the agreement is excellent!

The effect of arm dilution on crossbar dynamics is even more pronounced for the eight-arm A_3-**A**-A_2-**A**-A_3 architecture (samples P1508_8 and 1531_8). In this case, the dynamic regime intermediate between arm relaxation and terminal behavior is virtually nonexistent (Figure 6). If frictional drag is considered to be concentrated at three branch points, at least two complex Rouse modes should determine dynamics. The renormalized entanglement density of samples P1508_8 and 1531_8 is 10; cf. sample P1589 (Table 3). Furthermore, the larger number of friction centers per chain present in this polymer should yield a much slower escape from the renormalized tube. Yet the experimental results suggest a complete absence of a crossbar relaxation regime following arm retraction. The logical conclusion is that faster Rouse-like processes are responsible for molecular relaxation. On the basis of predictions for combs,[6] one would anticipate a Rouse time of the crossbar that is proportional to the square of number of branch points (eq 1). The terminal regime for P1508_8 should, therefore, be accessed at even lower frequencies than for its six-arm analogue. This is clearly opposite to what is seen experimentally. It is possible that a constraint release mechanism wherein arm relaxation (these on average comprise more than 6 out of every 10 crossbar entanglements for P1508_8 and 1531_8) so perforates the crossbar tube that the crossbar is effectively free after the arm constraints are lost. However, if this mechanism exists for the eight-arm polymers, it should also exist for all the six-arm materials, which is inconsistent with the large frequency range where crossbar relaxation dominates dynamics in six-arm polymers.

Even though the terminal relaxation behavior of eight-arm polymers, observed in linear oscillatory shear, is unusual, the long time step shear damping functions $h(\gamma)$ [$G(t;\gamma) = G_e h(\gamma)\, G(t)$, for $t > \lambda_k$, where λ_k is the separability time beyond which the nonlinear step shear relaxation modulus $G(t;\gamma)$ is separable into time and strain dependent parts] of these polymers are typical of the architecture supposed. Figure 8 compares the damping function $h(\gamma)$ observed using samples P1508_6 and P1508_8. The lower degree of strain softening seen in $h(\gamma)$ for 1508_8 is consistent with expectations for a change from a six-arm (pom-pom or A_n-**A**-A_n in general)[9,10] to eight-arm (comblike)[9] architecture. Details of the damping results of multiarm polymers will be the subject of a future paper.

The rich, but qualitative, insights into multiarm polymer dynamics provided by oscillatory shear data is evidently insufficient to pinpoint the relaxation dynamics of the crossbar. A more detailed consideration of how characteristic frequencies, time scales, and material properties depend on polymer molecular weight is of course possible. Thus, one could, for example, estimate a terminal or "reptation" time for the highly entangled materials (P1207 and P1589 from the crossover frequency [$\tau_{rept} \approx \tau_c \approx 1/\omega_c$]). From the reptation time and the storage modulus just before the onset of terminal behavior (G_{Rep}), a limiting shear viscosity η_0 can be estimated using the relation $\eta_0 \approx G_{Rep}\tau_{Rep}$. This approach is somewhat unconventional, and admittedly error prone, but is required because the terminal flow regime is never fully accessed in these slowly relaxing materials. We will see later, however, that the results compare favorably with a more rigorous approach based

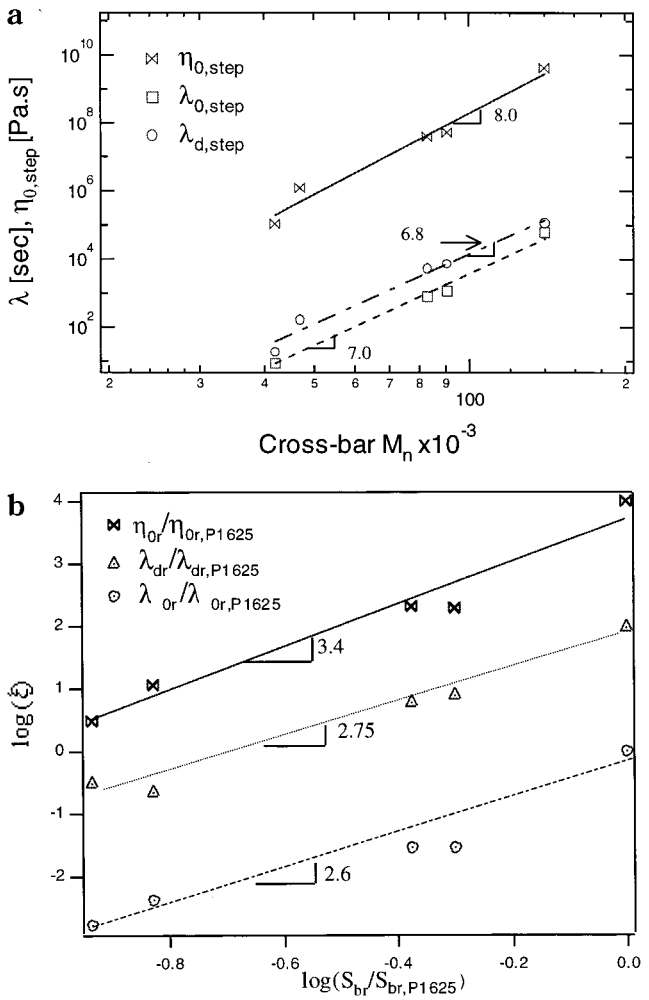

Figure 9. (a) Relaxation time and zero shear viscosity determined from step shear linear relaxation measurements as a function of crossbar molecular weight for A_3-**A**-A_3 polybutadiene. (b) Plot of reduced relaxation times and zero shear viscosities vs renormalized crossbar entanglement density for A_3-**A**-A_3 polybutadiene.

on direct measurements of the relaxation modulus $G(t)$ following small-amplitude step strain (Table 5).

In the case of polymers with lower renormalized crossbar entanglement density ($N_b\phi_b^{\alpha}/N_{eb0} \sim O(1)$), the terminal regime is fully accessed, but a clear plateau modulus is unobtainable. For these materials, a crossover relaxation time $\tau_c \approx 1/\omega_c$ and limiting shear viscosity η_0 can be readily obtained from the experimental results. As pointed out previously, other methods exist for calculating material properties. A longest molecular relaxation time λ_0 can, for example, be determined from the steady-state recoverable compliance ($\lambda_0 \approx \eta_0 J_e^0$), where the steady-state recoverable compliance is itself estimated from $J_e^0 = (1/\eta_0^2)\lim_{\omega\to 0}[G'(\omega)/\omega^2]$. A corresponding modulus, G_{long}, may also be calculated from J_e^0 ($G_{long} \approx 2.4/J_e^0$). As shown in Table 4, the longest relaxation time (λ_0) of linear polymer samples (PB129, PB1739, and PB1958) are the same order as the crossover time, τ_c ($\approx\omega_c^{-1}$). For multiarm samples where $N_b\phi_b^{\alpha}/N_{eb0} \sim O(1)$ (samples P1531–8, P1531–6, P1508–8, and P1508–6), λ_0 is consistently seen to be an order of magnitude higher than τ_c, suggesting the idea that the crossover is due to the relaxation of arms whereas λ_0 is associated with the relaxation of the entire molecule.

As mentioned before, low-amplitude step strain experiments provides yet another method for determining linear rheological properties of polymers. The terminal relaxation time can also be calculated from the long time slope of a semilogarithmic plot of $G(t)$ vs time ($G(t) \propto e^{-t/\lambda d,step}$). Table 5 summarizes material property data obtained from oscillatory shear and step shear measurements. In the limited number of cases where data could be obtained using both methods, results using the two approaches are seen to compare favorably.

Relaxation times ($\lambda_{0,step}$ and $\lambda_{d,step}$) and zero shear viscosity (η_0) for all six-arm polymers are plotted vs crossbar molecular weight in Figure 9a. Data for sample P1132 are also included from Archer and Varshney.[10] This sample has similar arm length (M_a = 19 500) to the polymers used in this study but has a different crossbar length (M_b = 47 000) to any of them. Best-fit lines provided in the figure suggest extremely strong power-law scaling dependences on crossbar M_n ($\lambda \propto M_b^{\sim 6.8-7}$, $\eta_0 \propto M_b^{\sim 8}$). At first glance these results would appear to rule out all but the slowest possible relaxation mechanism (arm retraction) for the crossbar. A more careful analysis of the experimental results is performed in terms of reduced material properties $\lambda_{dr} = \lambda_{d,step}/\tau_m$, $\lambda_{0r} = \lambda_{0,step}/\tau_m$, and $\eta_{0r} = \eta_0/\eta_m$, where $\tau_m \approx \omega_{max}^{-1}$ and $\eta_m \approx \zeta_m/b = kT\tau_m/b^3$, and renormalized crossbar entanglement density ($S_{br} = N_b\phi_b^{\alpha}/N_{eb0}$). Plotting the data in this way removes any crossbar molecular weight dependence of segmental scale properties and recognizes the dilution effect of relaxed arms (Figure 9b). For convenience all reduced/rescaled variables are also plotted as ratios with respect to data from the highest crossbar material. The best-fit lines suggest scaling relationships of the form $\lambda_{dr} \sim S_{br}^{2.6-2.8}$ and $\eta_{0r} \sim S_{b,r}^{3.4}$, results that appear somewhat stronger than expected for reptation relaxation mechanism for the crossbar.

Three possible sources can be identified for the higher than expected scaling exponents for a reptation dominated crossbar relaxation process (i.e., 2.8 compared to the expected values of 2): (I) Crossbar contour length fluctuations. In entangled melts and solutions of linear polymers, contour length fluctuations yield an increase of about 0.5 in the power-law exponent for the molecular weight dependence of terminal time and viscosity at intermediate molecular weights. As discussed in an earlier section of the article, our oscillatory shear results (i.e., broader G'' maxima and minima than in the case of linear polymers) point to a much greater role for fluctuations, possibly explaining our experimental observations. (II) Contribution from monomeric friction. The general expression derived earlier for the crossbar relaxation time includes a dependence on M_b.[3] This term will make a contribution to the crossbar relaxation time of order ($N_bN_e\tau_m/\tau_a$). For moderate crossbar molecular weights the contribution is small but grows linearly with crossbar molecular weight. (III) Crossbar effects on arm relaxation. As pointed out earlier, arm relaxation in a permanent network is slower than in a dynamic (diluted one). Slower relaxation of crossbar with increasing M_b therefore slows down arm relaxation in a potentially complex M_b-dependent way. McLeish et al.[7] have shown that this effect can in fact be captured in terms of their dynamic dilution proposal in terms of an effective concentration of "diluted" entanglement constraints. Their calculations in fact suggest a very strong, perhaps too strong, slowing down of arm relaxation time (e.g., by a factor of around $\exp[-2.5\alpha S_a(1-\phi_b)]$), for high

crossbar molecular weights), due to crossbar interference with arm relaxation.

Despite the uncertainty about the precise origin of the stronger crossbar molecular weight dependencies manifested by multiarm polymer properties, three conclusions can be drawn. First, the apparent increase in segmental relaxation time with crossbar molecular weight is likely real. Second, reptational diffusion is likely the dominant mechanism by which well-entangled crossbars relieve stress. Finally, the renormalized crossbar density is the correct molecular parameter for describing crossbar dynamics, which appears to further validate the dynamic dilution arguments of Ball and McLeish.[12]

Comparison of Experimental and Theoretical Oscillatory Shear Results. On the basis of the conclusions reached in the previous sections, it appears that the multiarm polymer theory of McLeish et al.[7] captures much of the physics governing six-arm polymer dynamics in the linear viscoelastic regime. It should therefore be possible to quantitatively predict the low-frequency (frequencies below the segmental and high-frequency Rouse regimes) dynamic results. Only two experimental parameters are in principle needed to make such a comparison: (i) the undiluted plateau modulus G_N of the polymer and (ii) the characteristic Rouse time for an entanglement segment, τ_e. As discussed earlier, the plateau modulus of linear 1,4-polybutadienes synthesized using the same methods employed for the multiarm materials yields an undiluted entanglement molecular weight $M_e = 1822$ g/mol. The Rouse time of an entanglement segment (τ_e) could in principle be estimated from the segmental relaxation time, but the numerical coefficients are not known precisely. We instead estimate it directly from the intersection of the rubbery plateau line for G' with the high-frequency Rouse regime.

Figure 10a−c shows a comparison of the experimental data with the model predictions of McLeish et al., taking G_N, τ_e, M_{ea}, and M_{eb} as adjustable parameters. The values of G_N, τ_e, and M_e used to obtain the fits are shown in these figures. The actual (estimated) values are also shown in parentheses. For entanglement molecular weight (M_{ea} and M_{eb}), a constant value of 2000 fits data best in the arm as well as in the crossbar relaxation regime. The values of G_N used to obtain the fits are within 50% of the actual ones, and the τ_e values are of the same order of magnitude as those determined from experiment. Considering the range of uncertainty in the estimated parameters, and the aforementioned deviations from classic Rouse frequency scalings observed in the experimental results, the correspondence between theory and experiment for the six-arm polymers can be considered fair.

A similar comparison of the experimental data with model predictions for one of the eight-arm polybutadiene samples (P1531_8) is shown in Figure 10c. The correspondence between theory and experiment is quite good in the arm relaxation regime. However, the crossbar shows much faster relaxation than predicted by the theory. Since the renormalized crossbar density is 10.6, the model predicts reptation as the longest relaxation mode of the polymer. This faster relaxation remains a puzzle because it rules out a reptation diffusion process, even though the diluted crossbars are well entangled. Indeed, polybutadiene molecules with A_3-**A**-A_2-**A**-A_3 architecture possess three friction centers per molecule and might therefore be expected to reptate even more slowly than their six-arm (A_3-**A**-A_3) counterparts; this expectation is not borne out by experiments, suggesting alternative relaxation processes must be considered. A more complete study of eight-arm materials with variable arm and connector molecular weights will shed light on these relaxation processes.

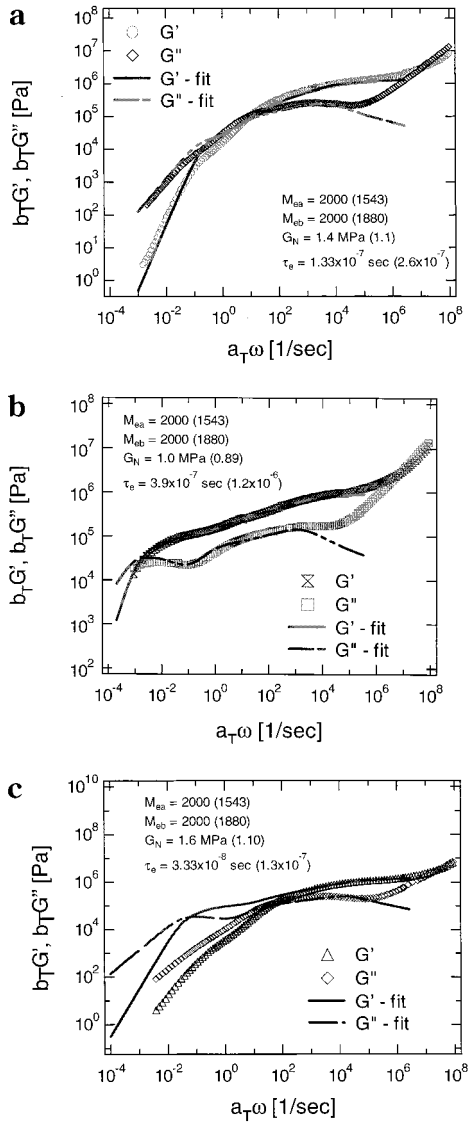

Figure 10. (a−c) Experimental data and predictions of tube model theory developed by McLeish et al.:[7] (a) A_3-**A**-A_3 polybutadiene with low crossbar length (sample P1508_6); (b) A_3-**A**-A_3 polymer with high crossbar length (sample P1589); (c) A_3-**A**-A_2-**A**-A_3 polybutadiene (sample 1508_8).

Phenomenological Description of Multiarm Polymer Dynamics. Next we turn to a more conventional, but phenomenological description of coupled dynamics in multiarm polymers. This description could provide additional insights into the origin of differences in relaxation dynamics of eight-arm and six-arm polymers. Figure 11, for example, plots the normalized imaginary component of complex viscosity (η''/η_0), where $\eta'' = b_T G'/(a_T\omega)$ for different polymer samples. For an entangled linear 1,4-polybutadiene (PB129), a single relaxation mode dominates the low-frequency spectrum. This mode is believed to result from reptational diffusion of individual molecules. The eight-arm polymer sample P1508_8 shows two relaxation modes. These modes are however quite broad and appear to merge into one, which is

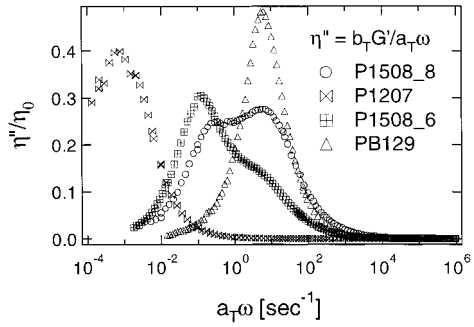

Figure 11. Normalized imaginary component of complex viscosity for linear and multiarm polybutadienes. For a simple Maxwell fluid $\eta''(\omega)/\eta_0$ has a maximum value of 0.4 at $\omega_c = \lambda_0^{-1}$.

consistent with a fluctuation dominated relaxation process. The corresponding data for the six-arm analogue of this same polymer also shows two relaxation modes. In this case, however, a clearer separation is apparent between the low-frequency cross bar relaxation and higher frequency arm relaxation. In fact, the dominance of the crossbar relaxation mode is so great that the higher frequency arm mode appears only as a kink in a broadened spectrum. Finally, in six-arm materials with large crossbar length (sample P1207), crossbar relaxation so dominate the spectrum that a clear arm relaxation regime is essentially nonexistent. The idea that one could model such a polymer as a single linear molecule with a rescaled (higher) molecular drag coefficient seems to be supported by these data.

It is possible to quantify some of these observations by fitting the experimental data to the KWW equation (eq 3). The fitting parameter β captures the breadth of the relaxation spectrum. The values of the stretch exponential exponent obtained for the segmental region (β_α) fall between 0.46 and 0.68 for the multiarm polymers, whereas for the linear polymers the values are between 0.69 and 0.75. The value of β_{arm} obtained for the arm relaxation by fitting eq 3 for the peak in G'' lies between 0.26 and 0.30 (Figure 12a). This value is much lower than the values of the stretch exponent reported for the terminal (~0.6) and segmental (0.4−0.5) regions.[16] The lower values of β_{arm} or higher values of n (0.74−0.8) suggests stronger cooperative interaction or coupling for arm relaxation compared to the coupling in the terminal and segmental regions of linear and multiarm polymers. Since the arm length of all the multiarm samples are about the same, the β_{arm} value of all the polymers are, as expected, quite similar.

Figure 12 shows the KWW fit for terminal and arm relaxation for two different multiarm polymers (sample P1531_8). The peak in G'' is not distinct and more importantly not symmetric. This observation is consistent with the anticipated broader relaxation spectrum and merging of the arm and segment relaxation regimes. The arm relaxation could in fact be argued to arrest the low-frequency end of the segmental relaxation. In the terminal region β_η value can be obtained only for multiarm samples P1207 and P1589. For these two samples, the crossbar is long enough so that the long time relaxation due to the slow diffusion of the crossbar is just accessible in our oscillatory measurements. The KWW fitting parameters for the G'' peak yield values for β_η 0.49 (P1589) and 0.55 (P1207). The corresponding coupling parameters (n) are 0.51 and 0.45, respectively. For the linear polybutadiene (PB129),

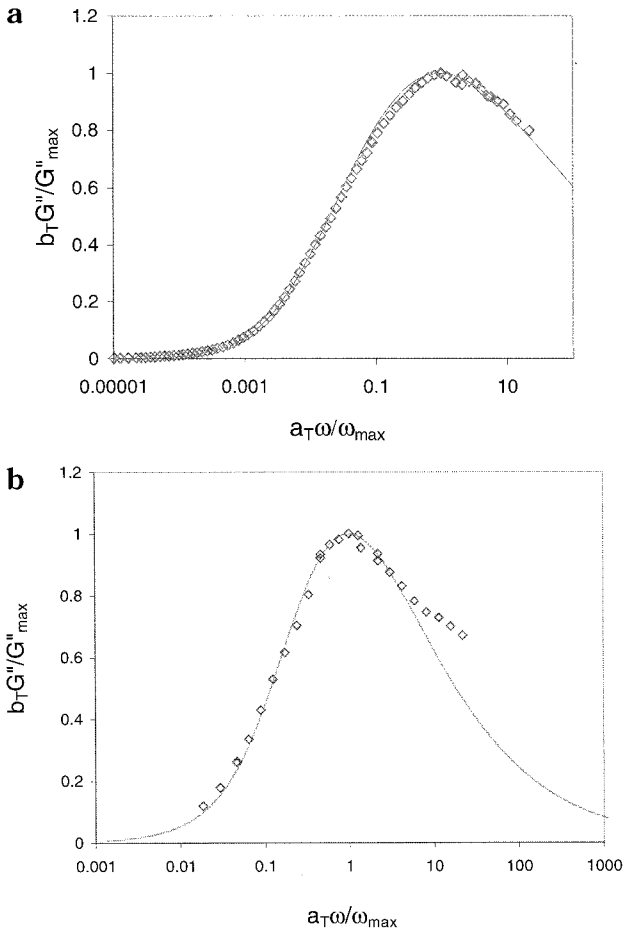

Figure 12. (a, b) Reduced loss moduli against reduced frequency and KWW fit in (a) the arm regime for sample P1531_8 ($\beta_{arm} = 0.27$) and (b) the terminal regime for sample P1207 ($\beta_\eta = 0.55$).

the β_η value obtained is 0.65. In the terminal zone Ngai model predicts a power-law dependence of zero shear viscosity (η_0) upon the molecular weight (M), $\eta_0 \propto M^{2/\beta\eta}$.[20] As linear polymers show a 3.4 exponent, the stretch exponent β_η is ~0.59. This value is independent of the polymer and is close to the experimental values.[14] The higher value of the coupling parameter (n) for multiarm polymers suggests more cooperative interaction among the crossbars of multiarm polymers due to the presence of arms.

Conclusions

Linear rheological properties of various model entangled six-arm (A_3-**A**-A_3) and eight-arm (A_3-**A**-A_2-**A**-A_3) polybutadiene melts are investigated using low-amplitude oscillatory shear and time-dependent step strain measurements. In oscillatory shear, the multiarm polymers generally show three peaks in loss moduli corresponding to segmental, arm, and crossbar relaxation; the low-frequency peak for the backbone relaxation is most evident for materials with high crossbar molecular weights. The mean segmental relaxation time of multiarm polymers is found to be a function of crossbar (**A**) molecular weight and polymer architecture. In materials with fixed arm (A) molecular weight, but variable crossbar molecular weight, terminal relaxation time (λ) and limiting shear viscosity (η_0) are observed to vary quite strongly with crossbar molecular weight M_b ($\lambda \sim M_b^{\sim 6.8-7}$, $\eta_0 \sim M_b^8$). However, when the crossbar tube

length is renormalized by dilution of relaxed arms and the relaxation time and viscosity are rescaled to remove the inherent M_b dependence of segmental scale properties, the scaling exponents are closer to values expected for fluctuating crossbar reptation in a dilated tube. Finally, the relaxation dynamics of eight-arm materials are found to be quite different from those of the six-arm polybutadienes. In particular, the slowest relaxation mode in well-entangled eight-arm (A_3-**A**-A_2-**A**-A_3) polymers appears to be dominated by Rouse-like fluctuation effects, which blur the transition from high-frequency arm to terminal backbone relaxation.

Acknowledgment. The authors are grateful to the National Science Foundation (Grants CMS-9713372 and DMR9816105) and to the Texas Higher Education Coordinating board for supporting this study.

References and Notes

(1) Small, P. A. *Adv. Polym. Sci.* **1975**, *18*, 1.
(2) Pearson, D. S.; Helfand, E. *Macromolecules* **1984**, *17*, 888.
(3) Milner, S. T.; McLeish, T. C. B. *Macromolecules* **1997**, *30*, 2159.
(4) Milner, S. T.; McLeish, T. C. B. *Macromolecules* **1998**, *31*, 7479.
(5) Roovers, J.; Graessley, W. W. *Macromolecules* **1981**, *14*, 776.
(6) Yurasova, T. A.; McLeish, T. C. B.; Semenov, A. N. *Macromolecules* **1994**, *27*, 7205.
(7) McLeish, T. C. B.; Allgaier, J.; Bick, D. K.; Bishko, G.; Biswas, P.; Blackwell, R.; Blotteiere, B.; Clarke, N.; Gibbs, B.; Groves, D. J.; Hakiki, A.; Heenan, R. K.; Johnson, J. M.; Kant, R.; Read, D. J.; Young, R. N. *Macromolecules* **1999**, *32*, 6734.
(8) Roovers, J. *Macromolecules* **1984**, *17*, 1196.
(9) McLeish, T. C. B.; Milner, S. T. *Adv. Polym. Sci.* **1999**, *143*.
(10) Archer, L. A.; Varshney, S. K. *Macromolecules* **1998**, *31*, 6348.
(11) Graessley, W. W. *Acc. Chem. Res.* **1977**, *10*, 332.
(12) Ball, R. C.; McLeish, T. C. B. *Macromolecules* **1989**, *22*, 1911.
(13) Colby, R. H.; Rubinstein, M. *Macromolecules* **1990**, *23*, 2753.
(14) Palade, L. I.; Verney, V.; Attane, A. M*acromolecules* **1995**, *28*, 7051.
(15) Ngai, K. L.; Plazek, D. J. *J. Polym. Sci., Polym. Phys. Ed.* **1985**, *23*, 2159.
(16) Zorn, R.; McKenna, G. B.; Willner, L.; Richter, D. *Macromolecules* **1995**, *28*, 8, 8552.
(17) Fetters, L. J.; Lohse, D. J.; Richter, D.; Witten, T. A.; Zirkel, A. *Macromolecules* **1994**, *27*, 4639.
(18) Ferry, J. D. *Viscoelastic Properties of Polymers*; Wiley: New York, 1980.
(19) Ziabicki, A.; Klonowski, W. *Rheol. Acta* **1975**, *14*, 113.
(20) Plazek, D. J.; Zheng, X. D.; Ngai, K. L. *Macromolecules* **1992**, *25*, 4920.

MA000892N